JOURNAL OF CATALYSIS 138, 223–239 (1992)

A ^{13}C NMR Study of Ethylene Adsorbed on Reduced and Oxygen-Covered Ag Surfaces

JUERGEN K. PLISCHKE, ALAN J. BENESI,* AND M. ALBERT VANNICE[1]

*Department of Chemical Engineering and *Department of Chemistry, The Pennsylvania State University, University Park, Pennsylvania 16802*

Received December 30, 1991; revised May 13, 1992

^{13}C-enriched ethylene was adsorbed on both clean and oxygen-covered Ag particles dispersed on η-Al_2O_3. Irreversibly adsorbed C_2H_4 on O-covered Ag exhibited an upfield shift of -20 ppm relative to gas-phase C_2H_4, whereas a narrower line and smaller shift of -5 ppm occurred for C_2H_4 reversibly adsorbed on reduced Ag. In addition to the resonance at 103 ppm for irreversibly adsorbed C_2H_4, CP/MAS NMR spectra also gave resonances at 179, 170, 164, 159, and 19 ppm for the O-covered Ag sample. The CP/MAS spectrum for Ag acetate powder clearly identified the 179- and 19-ppm peaks as those associated with the carboxyl and methyl carbons of the acetate anion, and the peaks at 159, 164, and 170 ppm were assigned to oxalate, formate, and carbonate (or possibly acetic anhydride) species, respectively, based on previous studies. When heated to 473 K the adsorbed C_2H_4 disappeared and only acetate and oxalate groups were observed, and continued heating to 573 K removed almost all resonances. No C_2H_4O was unambiguously detected, thus with this unpromoted Ag catalyst utilizing a high-surface-area alumina the observable surface species appeared to be those associated with complete combustion, with acetate and oxalate predominating during reaction. These results directly confirm the presence of an Ag acetate species which has been proposed previously to be an intermediate in complete combustion, and the presence of the other three species support earlier tentative assignments based on IR and TPR spectroscopy. Chemical shifts at 61, 28, and 13 ppm were indicative of alkoxy species formed on Brønsted-acid sites on the Al_2O_3 surface.

INTRODUCTION

The partial oxidation of ethylene over silver catalysts to form ethylene oxide is a well-studied reaction and has been the subject of numerous reviews (*1–6*). The elucidation of the reaction intermediates preceding epoxide formation versus those leading to complete oxidation products—CO_2 and H_2O—has been of principal interest. Commercial catalysts consist of large Ag particles dispersed on an α-Al_2O_3 support, and reaction mechanisms have been inferred from kinetic measurements on this system and Ag particles dispersed on other oxides such as η-Al_2O_3 and SiO_2 (*1*). Surprisingly, studies to identify surface species *under reaction conditions* are extremely scarce, and only the investigation of Force and Bell has reported the direct observation of reaction intermediates by using *in situ* infrared spectroscopy during ethylene oxidation over a Ag/SiO_2 catalyst (*7, 8*). However, even in their work some assignments were tentative and not confirmed, such as the proposal of oxalate and carboxylate species. More recent studies using well-defined Ag single-crystal surfaces have been informative as they were conducted using modern surface analysis techniques under UHV and controlled surface conditions (*1*); however, uncertainty can arise in extrapolating UHV results to practical reaction pressures. The most recent consensus in the open literature is that epoxidation proceeds by the reaction of C_2H_4 and atomic oxygen, both adsorbed on the Ag surface; reaction with oxygen bound weakly to the surface yields the epox-

[1] To whom correspondence should be addressed.

0021-9517/92 $5.00

ide, while a more strongly adsorbed form of oxygen leads to total combustion of C_2H_4 (*1*).

Nuclear magnetic resonance (NMR) spectroscopy can be a valuable tool to characterize species adsorbed on a surface (*9–16*), and NMR has recently been employed to study ethylene adsorption and reaction on Ru/SiO_2 (*17*) and SiO_2- and Al_2O_3-supported Pt (*18*). Magic-angle-spinning (MAS) NMR techniques provide another means by which stable reaction intermediates on a solid surface may be observed directly, and MAS NMR of ^{13}C nuclei in C_2H_4 is particularly attractive because the cross-polarization technique of magnetization transfer from abundant proton spins can be employed to enhance signal strength. Sensitivity is further improved through the use of C_2H_4 isotopically enriched in ^{13}C (natural abundance of ^{13}C is 1.1%). Thus, because of the limited direct information about surface species formed from coadsorbed oxygen and ethylene, we decided to apply this technique and determine what surface groups could be identified.

This study represents an application of high-resolution, solid-state NMR techniques including MAS, cross polarization, and high-power decoupling to examine the surface species formed at different temperatures after adsorption of C_2H_4 on a supported Ag catalyst. Samples of a pretreated $Ag/\eta\text{-}Al_2O_3$ catalyst were exposed to isotopically enriched $^{13}C_2H_4$ at room temperature and sealed in glass ampules for ^{13}C NMR experiments. These samples were encapsulated under either a chosen $^{13}C_2H_4$ partial pressure or a vacuum after removal of weakly adsorbed $^{13}C_2H_4$, and NMR spectra were acquired for samples containing $^{13}C_2H_4$ adsorbed on either clean or oxygen-covered Ag crystallites. The NMR spectra revealed the existence of both weakly adsorbed and more strongly bound C_2H_4 species on the Ag surface. In addition, evidence was obtained that stable carboxylate species, rigidly bound on the Ag surface, are produced via reaction of ethylene with adsorbed oxygen. These results are discussed in view of mechanisms that have been proposed in the literature for both partial and complete ethylene oxidation, especially since our catalyst is not expected to have high selectivity to ethylene oxide because it contains no promoters and it uses a high surface area alumina support (*1–3*).

EXPERIMENTAL

A 6.7 wt% Ag on $\eta\text{-}Al_2O_3$ catalyst was prepared by a standard incipient wetness technique (*19, 20*). The $\eta\text{-}Al_2O_3$ (245 m^2/g) was obtained from Exxon Research and Engineering Co. and had been prepared by the calcination in air of Davison β-alumina trihydrate for 4 h at 863 K. Prior to impregnation the support material was heated at 823 K for 2 h in air (Linde, dry grade) flowing at 0.472 l min^{-1} (STP) to remove any organic impurities. The appropriate amount of $AgNO_3$ (Aldrich Gold Label, 99.9999%) was dissolved in an amount of doubly distilled, deionized (DD) water which was just sufficient to fill the pore volume of the support, i.e., 0.5 ml H_2O/g Al_2O_3. The sample was dried in an oven overnight at approximately 373 K and stored in a desiccator. The Ag loading was determined by atomic absorption spectroscopy at the Mineral Constitution Laboratory of The Pennsylvania State University.

For adsorption isotherm measurements, ethylene (MG Industries, minimum purity 99.5%) was used with no additional purification. All other gases were ultrahigh purity (99.999%) and further purified prior to use by passing them through drying tubes (Supelco) and, except for O_2, Oxytraps (Alltech Associates). For adsorption measurements, catalyst samples were contained in Pyrex adsorption cells which permitted gas flow through the sample bed during pretreatment and were equipped with greaseless, high-vacuum stopcocks (Ace Glass), while samples prepared specifically for NMR experiments were treated in closed-end glass tubes. Both types of cells were attached to the adsorption apparatus via an FETFE O-

ring joint. Sample treatment and adsorption experiments were performed using one of two UHV stainless-steel adsorption systems, both of which provided a vacuum of 10^{-7} Torr at the sample (*20, 21*).

Sample pretreatment preceding isotherm measurements consisted of calcination in a flowing mixture of 10% O_2 + 90% He at 773 K for 2 h, evacuation at 673 K for 10 min, reduction in flowing H_2 at 673 K for 2.5 h, evacuation at 673 K for 10 min, and continued evacuation during cooling to the temperature desired for adsorption measurements. The subsequent adsorption scheme was as follows: (1) oxygen adsorption ($O_{2\,ADS}$) at 443 K, (2) evacuation at 443 K for 20 min and while cooling to room temperature, (3) ethylene adsorption ($C_2H_{4\,TOT}$) at room temperature, (4) evacuation at room temperature for at least 22 h, and (5) ethylene readsorption ($C_2H_{4\,REV}$) at room temperature. For ethylene adsorption measurements on clean Ag, the steps involving oxygen adsorption and evacuation at 443 K were omitted. Gas uptakes were corrected for physical adsorption by extrapolation of the isotherms to zero pressure by a least squares linear regression.

For NMR samples, ethylene isotopically enriched in ^{13}C at both carbon positions (MSD Isotopes, 99 atom% ^{13}C) was used with no additional purification. Adsorption was conducted with 50–150 mg samples in specially designed Pyrex closed-end cells (Wilmad) which could be flame-sealed to encapsulate $^{13}C_2H_4$-exposed samples in glass ampules which would fit inside a zirconia rotor with Kel-F endcaps. For pretreatment of the NMR samples in these closed-end tubes, O_2 was evacuated and replaced three times during the 2 h calcination at 773 K and H_2 was evacuated and replaced four times during the 2.5 h reduction at 673 K. The flame-sealing and separation of the ampule was typically performed with the aid of a variable-speed motor drive, and in some cases the tube was cooled in liquid N_2 prior to sealing to minimize the possibility of elevated temperatures. Details are provided elsewhere (*22*).

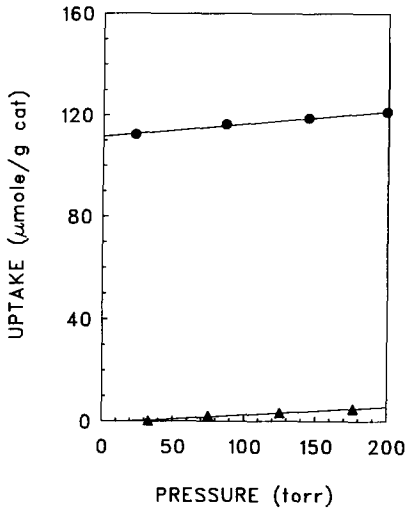

FIG. 1. Oxygen adsorption isotherms at 443 K for 6.7% Ag/Al_2O_3 (●) and pure Al_2O_3 (△).

^{13}C NMR spectra were obtained on a CMC-300A spectrometer operating at 74.78 MHz for ^{13}C (H_0 = 7.05 T) under both static (nonspinning) and magic-angle-spinning (MAS) conditions, and the ^{1}H resonance frequency was 297.38 MHz. The rf field strength for both was 50 kHz. Typical MAS speeds were ~5 KHz. Proton decoupled Bloch decay, cross polarization (CP), or cross polarization with interrupted decoupling (CP-ID) experiments were used to obtain ^{13}C spectra. All ^{13}C chemical shifts are reported relative to tetramethylsilane (TMS), and TMS resonance was determined from the chemical shift of the aromatic resonance of HMB (δ = 132.21 ppm). Typically 60,000 scans were acquired with a relaxation delay of 1 s for both Bloch decay and CP experiments. Variation of the relaxation delay from 1 to 10 s had no effect on the signal intensity for either experiment, indicating that the ^{13}C and ^{1}H T_1's were less than 0.3 s in all cases (except as noted in the text).

RESULTS

Reversible and irreversible uptakes of O_2 and C_2H_4 on the 6.7% Ag/Al_2O_3 and pure Al_2O_3 samples were determined from the isotherms shown in Figs. 1 and 2 (*22*), which

TABLE 1

Gas Uptakes on Ag Catalysts and Pure Supports after Reduction in Flowing Hydrogen

Sample	Gas uptake (μmol/g cat)			
	$O_{2\ ADS}$ 443 K	$C_2H_{4\ TOT}$ 298 K	$C_2H_{4\ REV}$ 298 K	$C_2H_{4\ IRREV}$ 298 K
6.7% Ag/Al_2O_3 (O_2-exposed)	111.4	219.5	141.7	77.8
6.7% Ag/Al_2O_3 (reduced)	Omitted	35.3	36.7	0
Al_2O_3	0	20.2	13.4	6.8

were measured after pretreatment of the samples under *flowing* gas conditions, and these results are listed in Table 1. Only irreversible oxygen adsorption occurred on the Ag surface, and oxygen adsorption at 443 K yields monolayer coverage on Ag (*19, 23, 24*). For ethylene adsorption data, $C_2H_{4\ TOT}$ represents the initial uptake and $C_2H_{4\ REV}$ represents the second uptake after evacuation at 298 K for 24 h. These results were used to determine the ratio of reversible to irreversible C_2H_4 adsorption on each catalyst after a specified pretreatment as well as the amount adsorbed on the pure alumina.

Gas uptakes on the encapsulated samples after *nonflowing* pretreatment conditions, as stated earlier, are summarized in Table 2. All samples were sealed at the specified C_2H_4 pressure, and the ratio of total atoms of adsorbed carbon to atoms of adsorbed oxygen (C_{AD}/O_{AD}) in each sealed ampule is also given. For oxygen-covered Ag/Al_2O_3, this value was near 2 for samples sealed under C_2H_4 but dropped to 0.74 after evacu-

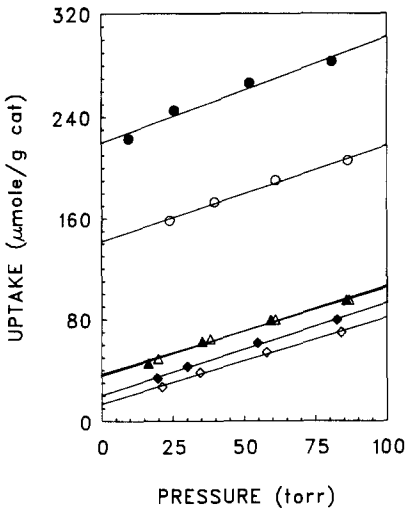

FIG. 2. Ethylene adsorption isotherms at 298 K for 6.7% Ag/Al_2O_3 and pure Al_2O_3. Closed symbols, $C_2H_{4\ TOT}$; open symbols, $C_2H_{4\ REV}$; (●, ○) oxygen-covered Ag/Al_2O_3, (▲, △) reduced Ag/Al_2O_3, (◆, ◇) pure Al_2O_3 blank.

TABLE 2

Treatment and Gas Uptakes for NMR Samples (Pretreatment with Nonflowing Gas)

Sample	Treatment $O_{2\ ADS}$ 443 K	Residual C_2H_4 pressure (kPa)	Gas uptake (μmol/g cat)		$\frac{C_{ad}}{O_{ad}}$[b]
			$O_{2\ ADS}$	$C_2H_{4\ ADS}$[a]	
6.7% Ag/Al_2O_3(R)	No	1.81	—	47.0	—
Al_2O_3(R)	No	1.91	—	12.6	—
Al_2O_3(O)	Yes	2.10	—	22.4	—
6.7% Ag/Al_2O_3(O)	Yes	1.62	79.6	167.4	2.1
6.7% Ag/Al_2O_3(O-E)	Yes	0[c]	81.5	60.3[d]	0.74

[a] Total uptake at specified C_2H_4 pressure.
[b] ($C_2H_{4\ ADS}/O_{2\ ADS}$) present after sealing.
[c] Sample evacuated after C_2H_4 adsorption.
[d] Irreversible C_2H_4 adsorption.

TABLE 3

Distribution of Adsorbed C_2H_4 in NMR Samples (from Tables 1 and 2)

Sample	Weight (mg)	μmol C_2H_4			
		Adsorbed on Ag		Adsorbed on Support	
		REV	IRREV	REV	IRREV
6.7% Ag/Al_2O_3 (R)	61.9	2.2	0	0.7	<0.1
6.7% Ag/Al_2O_3 (O)	62.2	5.9	3.2	1.0	0.2
6.7% Ag/Al_2O_3 (O-E)	130.3	0	7.4	0	0.5

ation of gas-phase and reversibly adsorbed C_2H_4. The 6.7% Ag/Al_2O_3(O), 6.7% Ag/Al_2O_3(R), and Al_2O_3(R) samples were cooled in liquid N_2 prior to sealing the ampule. The distribution of adsorbed C_2H_4 in each ampule was estimated using the $C_2H_{4\ ADS}$ uptakes in Table 2 plus the $C_2H_{4\ REV}/C_2H_{4\ IRREV}$ ratios on supported Ag and on the pure support from Table 1. It was assumed that the amount of C_2H_4 adsorbed on the η-Al_2O_3 support in each catalyst was the same (per g) as that on the pure support. The distribution of the C_2H_4 molecules in each sample is given in Table 3, and the percentage distributions are shown in Fig. 3. Even in samples with a residual C_2H_4 pressure, the amount of gas-phase C_2H_4 was typically less than 0.5% of the total; consequently, this C_2H_4 was neglected in the distribution calculations in Table 3 and Fig. 3.

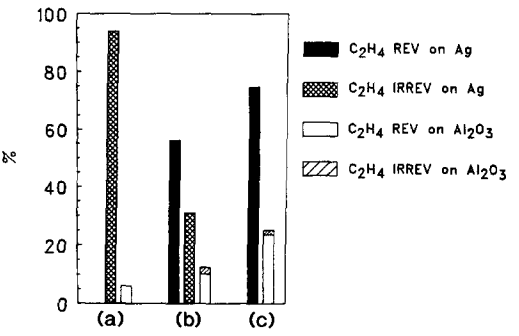

FIG. 3. Percent distribution of adsorbed C_2H_4 in NMR samples of 6.7% Ag/Al_2O_3: (a) 6.7% Ag/Al_2O_3(O-E), (b) 6.7% Ag/Al_2O_3(O), and (c) 6.7% Ag/Al_2O_3(R). See Table 2 for nomenclature.

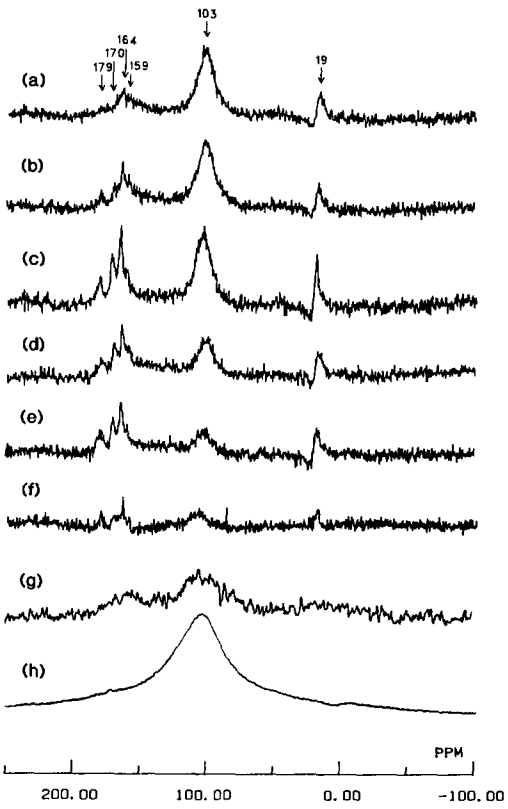

FIG. 4. ^{13}C CP/MAS NMR spectra of 6.7% Ag/Al_2O_3 (O-E): (a) CT = 0.2 ms; (b) CT = 0.5 ms; (c) CT = 1 ms; (d) CT = 2 ms; (e) CT = 4 ms; (f) CP-ID, CT = 1 ms, TAU = 50 μsec; (g) CP – nonspinning, CT = 1 ms, and (h) Bloch decay (with decoupling).

^{13}C spectra were acquired at 295 K for all samples in Table 2. Both cross polarization, magic-angle-spinning (CP/MAS) and single-pulse MAS spectra for 6.7% Ag/Al_2O_3(O-E) are shown in Figs. 4a–4e as a function of contact time (CT). The phase roll in Figs. 4a–4f is caused by left-shifting the free induction decay by 8–10 dwell units, which makes first-order phase correction difficult. Unlike the other samples, in order to spin the glass ampule containing 6.7% Ag/Al_2O_3 (O-E), it was necessary to wrap it with Teflon tape which gave two significant background resonances in ^{13}C CP/MAS spectra (150 ppm, $\Delta\nu_{1/2}$ = 80 ppm; and 28 ppm,

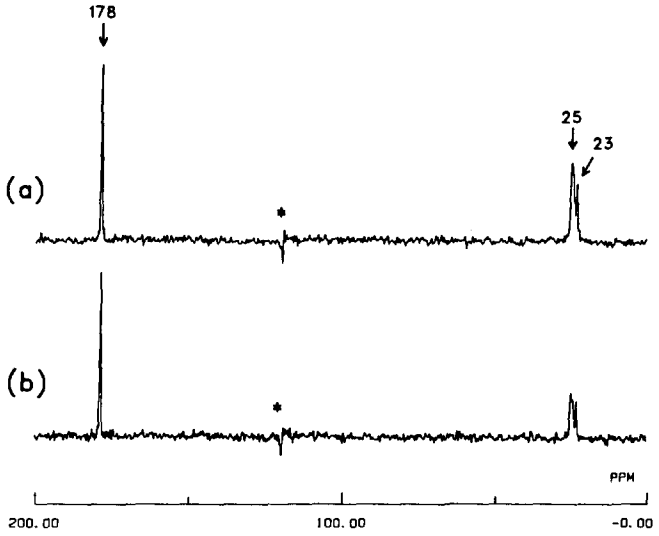

FIG. 5. ^{13}C CP-ID/MAS NMR spectra of silver acetate powder with two different decoupler delay times (TAU): (a) TAU = 10 μs and (b) TAU = 50 μs. Spinning sidebands are denoted by *.

$\Delta\nu_{1/2}$ = 20 ppm). The ^{13}C CP/MAS spectrum of Teflon tape was also obtained (not shown) and this was fractionally subtracted from the spectra of the sample to yield difference spectra virtually identical to those in Figs. 4a–4f. Whether the FID is left-shifted prior to Fourier transformation or the spectra are subtracted, an apparent phase anomaly occurs on the downfield side of the resonance at 19 ppm. For the nonspinning spectrum of 6.7% Ag/Al_2O_3(O-E) in Fig. 4g, and for all the other NMR samples, no Teflon tape was used. The maximum signal intensity was obtained with CT = 1 ms, and this value was used in all other cross-polarization experiments. A Bloch decay for this sample is shown in Fig. 4h. Based on a relative signal to noise comparison of the fully relaxed spectra in Figs. 4c and 4h, approximately 6% of the NMR observable, irreversibly bound ^{13}C was cross-polarizable assuming no significant CP enhancement.

The resonances at 179, 170, 164, and 159 ppm are in the normal range of carboxyl or carbonate shifts (*25–27*), and those at 179 ppm and 19 ppm are entirely consistent with the carboxyl and methyl carbons of the acetate anion in the solid state, as shown by the spectrum of

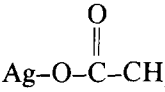

in Fig. 5. Further confirmation is provided by the study of Chin and Ellis, in which resonances at 180 and 19 ppm for acetic acid on Ag/Al_2O_3 were reported (*26*). The resonance at 164 ppm is the same as that observed for solid ammonium formate at 185 K (*25*), and it is near that of 168 ppm reported for formic acid on Ag/Al_2O_3 (*26*); thus we assign this reasonance to the formate anion. The resonance at 159 ppm is near that reported for oxalic acid on Ag/Al_2O_3 (*26*) and is assigned to the oxalate anion. Finally, the resonance at 170 ppm is the same as that for $BaCO_3$; however, solid acetic anhydride has a chemical shift of 171 ppm (*25*). It might be argued that the carbonate species would not be observed in the CP/MAS spectrum because they contain no protons; however, the close proximity of coadsorbed species such as ethylene or acetate would allow cross polarization and the presence of this peak. Finally, although the observable species appear to be on the Ag, we cannot disallow the possibility that one or two of these four peaks could represent an acetate or oxalate species residing in a

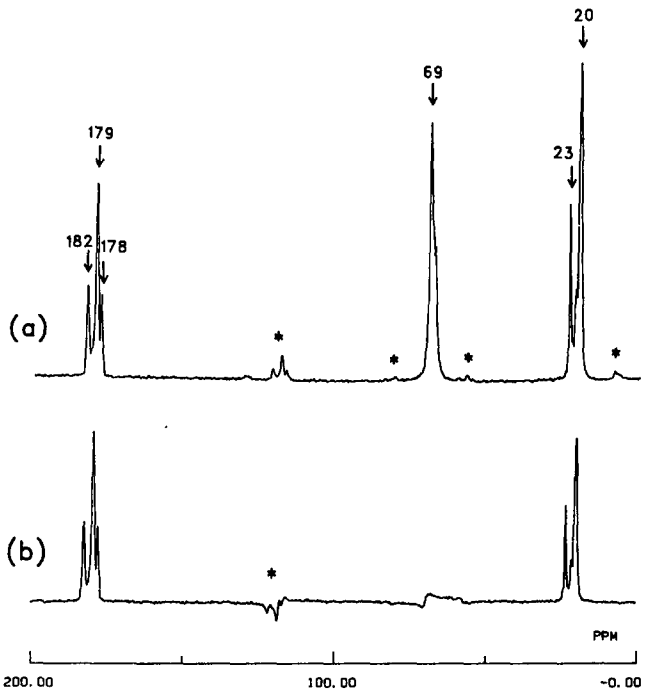

FIG. 6. ^{13}C CP-ID/MAS NMR spectra of silver lactate powder with two different decoupler delay times (TAU): (a) TAU = 10 μs and (b) TAU = 50 μs. Spinning sidebands are denoted by *.

different microenvironment, such as being adsorbed on the Al_2O_3 surface in addition to the Ag surface. That a carboxyl group or a methyl group within a molecular ion can give rise to multiple resonances is demonstrated in Fig. 6 for silver lactate,

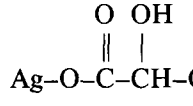

Such variations may arise from different microenvironments within the unit cell of a crystal, from different solid phases, or from the state of protonation of the carboxyl group. In Fig. 4, the resonance at 103 ppm is that of irreversibly adsorbed ethylene on an oxygen-covered Ag surface. It is shifted upfield from the resonance expected for gas-phase ethylene, which is 119–123.5 ppm (*27–29*).

The observation of the small fraction of the ^{13}C-containing species in Fig. 4 with cross polarization indicates that for these species the motion is sufficiently limited to allow the dipolar interaction to be used to transfer polarization from protons to ^{13}C. Anisotropic motion is evident, even in the CP spectra, because they do not exhibit the expected spinning sidebands for ethylene or carboxyl species (*25, 26*). Conversely, the inability to observe 94% or more of the ^{13}C by cross polarization indicates either that most of the ^{13}C atoms are undergoing isotropic motion, or that there are no protons in the vicinity, or that these ^{13}C atoms are rapidly exchanging hydrogen. Cross polarization does not work for molecular groups undergoing rapid isotropic motion in the liquid and gaseous states; however, the absence of spinning sidebands, ($\nu_{rot} \sim 5$ KHz) for the carboxyl and ethylene resonances indicates that significant anisotropic motion must be occurring at 295 K. The chemical shift tensor for ethylene spans about 200 ppm (*25, 26*), and the tensors for carboxyl and carbonate species span at least 140 ppm (*25*); hence, one would expect to observe spinning sidebands for those species if they

were rigidly bound. The nonspinning CP spectrum obtained for 6.7% Ag/Al_2O_3(O-E) in Fig. 4g is consistent with the hypothesis of anisotropic motion. Both the carboxylate (and carbonate) and ethylene resonances broaden with no spinning, but both are considerably narrower than would be expected from their chemical shift tensors if they were rigidly bound.

The interrupted decoupling or dipolar dephasing experiment (CP-ID/MAS) suppresses resonances from protonated ^{13}C nuclei which do not undergo sufficient motion to reduce the ^{13}C–^{1}H dipolar interaction (*30*). Protonated ^{13}C nuclei which undergo rapid anisotropic motions, such as the methyl groups in Figs. 4f, 5b, and 6b, have a dipolar interaction which is sufficiently reduced to allow their resonances to survive a delay of 50 μs. Although irreversibly adsorbed, the ethylene in Fig. 4f also must experience considerable anisotropic motion at 295 K because its resonance also survives the 50-μs delay. There is a slight downfield shift of the C_2H_4 peak towards that for the reversibly adsorbed C_2H_4, as expected for less strongly bound C_2H_4. The methyne (C–H) resonance of silver lactate (Fig. 6) does not survive this delay, indicating rigid conformation at room temperature. The quaternary carboxyl or carbonate resonances in Fig. 4f are expected to persist with or without anisotropic motion. If the formate ion is on the surface, it must undergo motion because its presumed resonance at 164 ppm survives the 50-μs delay.

Notably absent from any of the spectra for 6.7% Ag/Al_2O_3 (O-E) in Fig. 4 is a resonance for ethylene oxide, which would be expected between 40 and 70 ppm (*25*) and has been reported at 61 ppm on O-covered Ag (*26*). This absence may be due to low signal-to-noise, the Teflon tape background, or it may reflect an underlying difference between the chemical fates of irreversibly bound ethylene and more weakly bound ethylene. Also absent is any sign of the ^{13}C–^{13}C homonuclear dipolar coupling between ^{13}C nuclei in ethylene (*26*). Again, magic angle spinning and anisotropic motion at 295 K average this interaction, but it may contribute to the broadening observed for irreversibly bound ethylene in the non-spinning spectrum.

In Fig. 7a, the ^{13}C CP/MAS spectrum for the Al_2O_3(R) sample (Table 2) reveals four resonances. The resonance at 123 ppm represents weakly adsorbed ethylene. The chemical shift is close to that observed for gas-phase ethylene, unlike the shift observed for ethylene adsorbed on a Ag surface (Figs. 7b–7e). The adsorbed ethylene is cross-polarizable but does not yield spinning sidebands; therefore, it too must experience anisotropic motion. The resonances at 61, 28, and 13 ppm are attributed to alkoxy species, such as $Al–O–CH_2–CH_3$ and $Al–O–CH_2(CH_2)_2–CH_3$, which are most likely associated with Brønsted-acid sites (*31*). These shifts are in the expected ranges for –O–C–(70–50 ppm),–CH_2–(40–20 ppm), and –CH_3(20–0 ppm) groups (*27*). Carboxyl or carbonate resonances are notably absent from the spectrum. No ^{13}C resonance was observed for the Al_2O_3(O) sample after exposure to $^{13}C_2H_4$.

Figure 7b is the ^{13}C CP/MAS spectrum of C_2H_4 adsorbed on a clean, reduced Ag surface (Sample 6.7% Ag/Al_2O_3(R), Table 2). The strong resonance at 118 ppm is significantly upfield from gaseous ethylene or the ethylene weakly adsorbed on Al_2O_3(R). Interaction with the silver is evident. The residual peak at 13 ppm probably represents methyl groups of aluminum alkoxide species, such as that found in Al_2O_3(R) (Fig. 7a). No carboxyl or carbonate resonances are present.

In Fig. 7c, the CP/MAS spectrum reveals a further upfield shift to 111 ppm for the ethylene adsorbed on an O-covered Ag surface, the presence of acetate resonances at 181 and 20 ppm, the presence of oxalate at 161 ppm, residual aluminum alkoxide resonances at 30 and 13 ppm, and a resonance at 61 ppm which is most likely an aluminum alkoxide species even though ethylene oxide has been reported to have a resonance

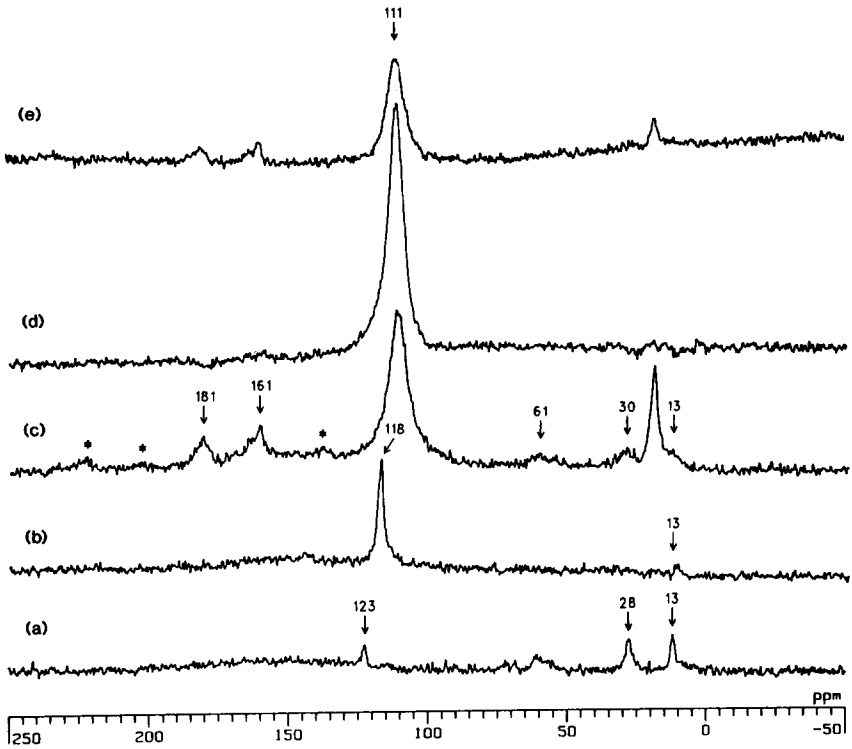

FIG. 7. ^{13}C spectra of C_2H_4 adsorbed on samples from Table 2: (a) CP/MAS of Al_2O_3(R), CT = 1 ms; (b) CP–MAS of 6.7% Ag/Al_2O_3(R), CT = 1 ms; (c) CP/MAS of 6.7% Ag/Al_2O_3(O), CT = 1 ms; (d) Bloch decay (with decoupling) of 6.7% Ag/Al_2O_3(O); and (e) CP-ID/MAS of 6.7% Ag/Al_2O_3(O), CT = 1 ms, TAU = 50 μsec. Spinning sidebands are denoted by *.

at 61 ppm on an O-covered Ag surface (*26*). The resonances marked by an asterisk are spinning sidebands of the carboxylate peaks, as verified by changing the spin rate. The ethylene peak at 111 ppm is considerably broader than that observed for the reduced samples but narrower than that observed for irreversibly adsorbed ethylene on an O-covered Ag surface (Table 4). Spectra of a similar sample obtained with a Chemagnetics M100S spectrometer using a Delrin rotor also produced resonances at 162 and 111 ppm, but resonances from the rotor overlapped the other regions of interest (*22*).

When compared to the CP/MAS spectrum in Fig. 7c, the proton decoupled Bloch spectrum of 6.7%/Al_2O_3(O) in Fig. 7d reveals that about 85% of the ethylene in this sample is not cross-polarizable due to fast exchange and/or motion. Experiments in which the relaxation delay was varied by a factor of 10 revealed no change in the observed signal to noise, indicating that relaxation was complete for the adsorbed ethylene. The CP-ID/MAS spectrum of 6.7% Ag/Al_2O_3(O) in Fig. 7e shows that the ad-

TABLE 4

Chemical Shift (δ) and Linewidth (Δf) for C_2H_4 Adsorbed on 6.7% Ag/Al_2O_3 Catalysts

Sample—Form of C_2H_4	δ (ppm)[a]	Δf[b]	
		Hz	ppm
(O-E)—Irrev. on O-covered Ag	103	1030	13.8
(O)—Irrev. + rev. on O-covered Ag	111	610	8.2
(R)—Rev. on clean Ag	118	200	2.7
Al_2O_3 (R)—Rev. on Al_2O_3	123	150	2.0
Gas-phase C_2H_4	123.5[c]	—	—

[a] Relative to TMS.
[b] Full linewidth measured at half-height.
[c] From Ref. (*27*).

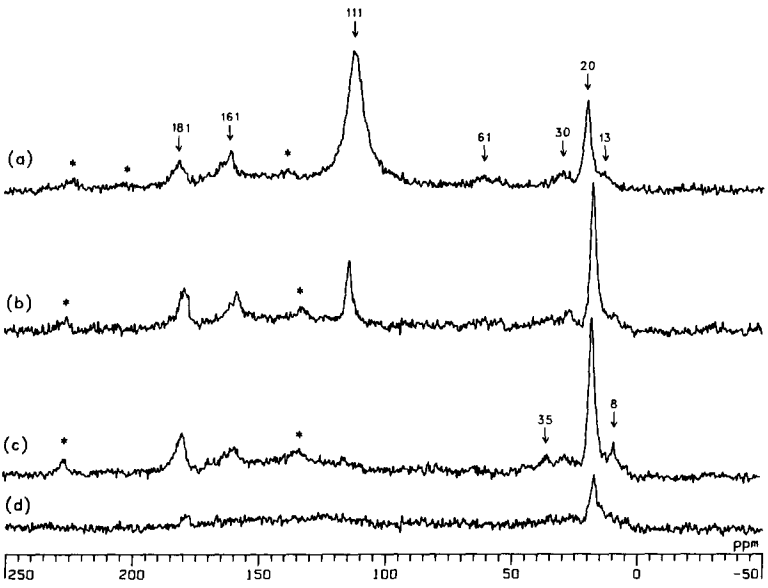

FIG. 8. ^{13}C CP/MAS NMR spectra of the 6.7% $Ag/Al_2O_3(O)$ sample at 298 K after heating at successively higher temperatures: (a) t = 298 K, (b) T = 473 K, (c) T = 523 K, and (d) T = 573 K. Spinning sidebands are denoted by *.

sorbed acetate, oxalate, and ethylene species undergo substantial anisotropic motion, while the alkoxide (and possibly ethylene oxide) resonances do not.

The effect of heating for 15 min at successively higher temperatures is shown by the CP/MAS spectra in Fig. 8 for the $Ag/Al_2O_3(O)$ sample. The intensities of the ethylene and alkoxide resonances are greatly reduced after 15 min at 473 K, and both are gone after 15 min at 523 K, although new resonances appear at 35 and 8 ppm after this treatment. These may be due to oligomers of ethylene, as discussed later. The oxalate is somewhat reduced after 15 min at 523 K, and after an additional 15 min at 573 K only a weak acetate resonance remains.

DISCUSSION

There is a pronounced scarcity of studies related to the *direct* observation of surface intermediates formed by coadsorbed oxygen and C_2H_4 on Ag, especially under reaction conditions. Only the IR study of Force and Bell has been conducted during reaction (*7*, *8*), although Gerei *et al.* (*32*) and Kilty *et al.* (*33*) provided limited IR spectra after adsorbing C_2H_4 on O-covered Ag surfaces at 95°C and heating to temperatures above 110°C. The conclusion reached in the latter two papers was that a peroxide species was formed at the lower temperature which converted to an alkoxide species above 110°C (*32*, *33*). Force and Bell also saw IR bands attributable to alkoxide species, but in addition they identified carbonate groups and they observed bands that were tentatively assigned to a carboxylate structure and to an oxalate species (*7*). Both of the latter were associated with complete combustion products (*7*). Kanno and Kobayashi used a transient response method to react either H_2 or O_2 with surface species formed during C_2H_4 oxidation, and they concluded that an acetate species was the most probable (*34*). The presence of an acetate species on an O-covered Ag(110) surface was also indicated by the work of Barteau *et al.*, and they also

proposed the possibility of a surface anhydride species (*35*). Our results provide support for the formation of some of these species but not others; however, first we discuss the adsorbed ethylene species.

Adsorbed Ethylene

The NMR spectra obtained in this study verify the existence of adsorbed C_2H_4 species, $(C_2H_4)_{AD}$, on both the alumina and the Ag surface. The strength of the adsorptive bond and the nature of the adsorption site depend on the substrate and the surface conditions. The chemical shifts of C_2H_4 adsorbed on the different Ag/Al_2O_3 samples and the pure Al_2O_3 are given in Table 4. The shifts range from 103 ppm for irreversibly adsorbed C_2H_4 on oxygen-covered Ag to 123 ppm for C_2H_4 adsorbed on pure Al_2O_3, thus corresponding to chemical shifts up to -20 ppm with respect to gas-phase C_2H_4. Previous studies have shown that this variation in chemical shift reflects the strength of interaction of C_2H_4 with the substrate (*36–39*). The ^{13}C chemical shifts of adsorbed ethylene are particularly sensitive to the presence of Ag^+ ions. For example, Meiler *et al.* (*36*) obtained NMR spectra of ethylene adsorbed in various cation-exchanged zeolites and found that only for unreduced AgNaX zeolites was the NMR peak shifted upfield (i.e., to lower ppm values) with respect to the gaseous state. Shifts up to -7.8 ppm were reported for AgNaX (60% Ag^+). The spectra of Michel *et al.* for 1-butene adsorbed in AgNaX zeolite and 1-butene dissolved in ionic solutions of $AgNO_3$ or $AgBF_4 \cdot H_2O$–$CHCl_3$ were identical, and each spectrum exhibited line shifts near -12 ppm with respect to the gaseous state (*37*). These effects were attributed to the preferred formation of Ag^+–olefin complexes in zeolites with the terminal $=CH_2$ groups localized near Ag^+ ions. Analogous behavior was observed by Takasugi *et al.* in their spectra of 1-alkenes adsorbed on $AgNO_3$-impregnated SiO_2 which had been dried *in vacuo* at 333 K for 6 h (*39*). Terminal $=CH_2$ groups exhibited chemical shifts of -9.8 to -12.8 ppm (relative to pure liquid) for 1-pentene, 2-hexene, 1-heptene, and 1-octene adsorbates, whereas negative shifts of less than 1 ppm were observed on pure SiO_2. These authors also concluded that the carbon–carbon double bond forms a π-complex with surface Ag^+ ions, which explained the difference in chemical shift reported for ethylene adsorbed on NaY (δ = 124 ppm) and AgY zeolites (δ = 115 ppm) (*27*). This same conclusion was reached by Chin and Ellis (*26*). Force and Bell (*7*) found that the IR spectra of C_2H_4 adsorbed on oxygen-covered Ag/SiO_2 catalysts closely resembled those reported for Ag^+–C_2H_4 complexes in zeolites; consequently, they concluded that the probable adsorption sites are Ag^+ ions in a silver oxide surface layer where chemisorbed oxygen exists in the form of negative ions.

The linewidths of the $(C_2H_4)_{AD}$ peak in each sample are also given in Table 4, and the trend toward narrower lines parallels the downfield shift in line position. NMR linewidths provide qualitive information on the mobility of adsorbed C_2H_4. As shown by Chin and Ellis (*26*), the resonance line of rigidly bound C_2H_4 molecules will exhibit the convolution of chemical shift and homonuclear ^{13}C–^{13}C dipolar effects; however, if C_2H_4 is sufficiently mobile on the surface, the individual ^{13}C spins will experience only the average of the local fields and the line will narrow. Thus, from the data in Table 4, it may be concluded that the degree of C_2H_4–substrate interaction becomes greater as both the chemical shift decreases and the linewidth increases.

Based on these observations, the following conclusions can be reached about the nature of the adsorbed C_2H_4. The irreversibly adsorbed C_2H_4 on oxygen-covered Ag (δ = 103 ppm) is the most strongly bound and, since it exists only in the presence of adsorbed oxygen, it may be associated with surface sites containing Ag^+ cations which are created by adsorbed oxygen. In the absence of adsorbed oxygen, only reversibly adsorbed C_2H_4 (δ = 118 ppm) is present,

and over 75% of the C_2H_4 is associated with the reduced Ag surface with the remainder adsorbed on the Al_2O_3 (see Table 3). This weak adsorption on reduced Ag is consistent with both the work of Force and Bell (*7*), in which IR spectra of adsorbed C_2H_4 were not observed in the absence of oxygen, and a recent calorimetric study in our laboratory of C_2H_4 adsorption on Ag/Al_2O_3 catalysts which measured much higher heats of adsorption (Q_{AD}) on O-covered Ag (*40*). In addition, the relative strength of adsorption is consistent with C_2H_4 Q_{AD} values of 8.9 and 10.7 kcal/mol reported by Campbell and Paffett for clean and oxygen-covered Ag(110) surfaces, respectively (*41*). When both irreversibly and reversibly adsorbed C_2H_4 are present in a Ag sample which had been exposed to oxygen, an intermediate chemical shift (δ = 111 ppm) is observed. It is reasonable to assume that in the presence of oxygen, the resonance line for reversibly adsorbed C_2H_4 would also exhibit a downfield shift relative to the irreversibly adsorbed phase. This suggests that the single broad line at 111 ppm is actually a multitude of different NMR lines due to the ethylene in exchange at different rates between adsorption sites of varying strength. Both reversibly and irreversibly adsorbed states possess mobility on the Ag surface with the irreversibly adsorbed state obviously being the less mobile of the two. The weakest interaction occurs on the pure Al_2O_3 sample (δ = 123 ppm), where most of the small quantity of C_2H_4 present is reversibly adsorbed, and the chemical shift is essentially that of the gaseous state. This is consistent with a chemical shift of 123 ± 1 ppm recently reported for C_2H_4 weakly adsorbed on SiO_2 (*17*). The strength of the surface interaction also parallels the total C_2H_4 uptakes of 167.4, 47.0, and 12.6 (μmole/g cat) in Table 2 for oxygen-covered Ag, reduced Ag, and pure Al_2O_3, respectively.

In contrast to these results, C_2H_4 adsorbed on reduced Ru/SiO_2 (*17*) or on reduced Pt/SiO_2 or Pt/Al_2O_3 (*18*) was not detected by NMR because C_2H_4 reacted with these surfaces at room temperature; consequently, only adsorbed reaction products were detected. On reduced Ru/SiO_2 at room temperature, adsorbed C_2H_4 decomposed to form strongly adsorbed acetylide and alkyl groups; in addition, weakly adsorbed ethane, butane, and butene were formed via recombination of adsorbed species and hydrogenation of ethylene (*17*). At room temperature, ethylene adsorbed on reduced Pt/SiO_2 or Pt/Al_2O_3 formed a π-bonded olefin complex, and for samples containing Al_2O_3 or Cl^-, this complex reacted to form σ-adsorbed vinyl groups and surface alkyls (*18*).

The conclusion that $(C_2H_4)_{AD}$ is mobile on the surface of oxygen-covered Ag was confirmed by a number of experiments. A comparable drop in signal intensity with increasing contact time was observed for both reversibly and irreversibly adsorbed C_2H_4 (see Figs. 4 and 7). This behavior is consistent with a relatively short $T_{1\rho}$ relaxation time commonly associated with molecular motion, which results in the CP technique becoming ineffective for systems in which $T_{1\rho}$ is unusually short or T_{CH} is very large (*42*). The fact that magic angle spinning produced no change in lineshape for the sample containing both irreversibly and reversibly adsorbed C_2H_4 is also consistent with adsorbed C_2H_4 possessing mobility on an oxygen-covered Ag surface. In addition, the loss of a detectable signal at low temperature (193 K) under otherwise identical conditions indicates decreased mobility which broadened the NMR line beyond detection capability under nonspinning conditions (*22*). The slight broadening of the line for irreversibly adsorbed C_2H_4 in the nonspinning spectrum obtained at 295 K (see Fig. 4) indicates anisotropic motion for this species. Anisotropic motion also accounts for the presence of the $(C_2H_4)_{AD}$ peak in the CP spectra acquired with interrupted decoupling. These results are completely consistent with those reported by Chin and Ellis (*26*).

Adsorbed Reaction Products

The NMR spectra reveal that exposure of C_2H_4 to an oxygen-covered Ag surface produced species other than just adsorbed C_2H_4; however, these additional species were not formed on a reduced Ag surface, i.e., the 6.7% $Ag/Al_2O_3(R)$ sample, which shows that they result from a reaction between C_2H_4 and adsorbed oxygen. It should be emphasized that the concentrations of the reaction products in Fig. 7c are small when compared to the concentration of $(C_2H_4)_{AD}$, as suggested by the relative peak intensities. In the CP/MAS spectra of the 6.7% $Ag/Al_2O_3(O)$ and 6.7% $Ag/Al_2O_3(O\text{-}E)$ samples (Figs. 4 and 7), predominant peaks occur near 20 ppm and between 159 and 181 ppm. A 20-ppm chemical shift lies well within the range associated with aliphatic carbons and most closely resembles the chemical shift of a methyl group ($-CH_3$), and the downfield peaks occur in the range of carboxylic and carbonate carbons (*25–27*). These resonances originate from species strongly bound to a surface since they are present even after gas-phase evacuation at 298 K for 24 h.

With both weakly and strongly bound C_2H_4 adsorbed on an O-covered Ag surface, which gave the higher C_{AD}/O_{AD} ratio of 2.1 for 6.7% $Ag/Al_2O_3(O)$ in Table 2, only acetate and oxalate (and possibly ethylene oxide) species exist on the Ag surface (Fig. 8). This sample had been placed in liquid N_2 prior to sealing it off; therefore, any heating of the system during seal-off would have been minimized. Under these conditions, the C–C bond remains intact although strong C=O and C–O bonds are created. When only irreversibly adsorbed C_2H_4 was present on such a surface, thus giving the lower C_{AD}/O_{AD} ratio of 0.74 for 6.7% $Ag/Al_2O_3(O\text{-}E)$ in Table 2, formate and carbonate species were also formed. We do not know at this time whether these additional reactions are due primarily to the presence of only the more strongly bound C_2H_4 species, to the higher O_{AD}/C_{AD} ratio, or to a greater extent of heating because this sample was not cooled in liquid N_2 prior to seal-off. However, the absence of any distinct resonances near 166 and 172 ppm (assuming a 2-ppm drift in these spectra) implies that one of the former explanations dominates—perhaps the excess oxygen present allows more complete oxidation to occur in the sample shown in Fig. 4. The fact that all downfield resonances are retained in a CP-ID experiment (Fig. 4g) indicates that either all species have a C atom not bonded to a hydrogen atom or they are not rigidly bound. This could imply that no acetaldehyde is present because this molecule contains a C–H bond.

In studies of the oxidation of ethylene to ethylene oxide and also of acetaldehyde over Ag catalysts, an adsorbed acetate species has been proposed as an intermediate responsible for complete oxidation to CO_2 and H_2O (*7, 8, 34, 35, 43, 44*). It is known that ethylene oxide can isomerize to acetaldehyde over Ag or Al_2O_3 and that acetaldehyde can be a by-product during the partial oxidation of C_2H_4 to C_2H_4O (*1, 45, 46*). Madix and co-workers (*35*) investigated the adsorption of acetaldehyde on an oxygen-dosed Ag (110) surface using temperature-programmed spectroscopy and found that adsorption at 300 K appeared to produce a stable adsorbed acetate species and gas-phase H_2. The adsorbed acetate complex was stable up to 640 K in vacuum, at which temperature it decomposed to yield CO_2, CH_3COOH, CH_4, H_2C_2O, and atomic carbon residues. Force and Bell reported the observation of a –COO– functional group present in an adsorbed species under reaction conditions for ethylene oxidation at 693 K. Their evidence consisted of an IR band at 1740 cm^{-1} which was associated with the vibration of the C=O bond in a carboxylate group. In a later paper, these same authors proposed that the carboxylate was part of an acetate intermediate adsorbed on Ag and that formation of this species precedes the formation of CO_2 and H_2O (*8*). A plausible pathway to form an adsorbed acetate species on Ag involves the reaction of C_2H_4

with an adsorbed oxygen atom to form ethylene oxide, which subsequently isomerizes to acetaldehyde. For example, Grant and Lambert (*46*) reported an isomerization rate of 8×10^{14} molecules s^{-1} cm^{-2} on an Ag(111) surface at 300 K. The formation of adsorbed acetate is presumed to occur by a mechanism similar to that proposed by Madix and co-workers (*35*), i.e., the acyl carbon of acetaldehyde is subjected to nucleophilic attack by an adsorbed oxygen atom, and the subsequent loss of a hydrogen atom yields the adsorbed acetate structure. *Our results provide confirmation that an Ag acetate species is indeed formed on unpromoted, O-covered Ag surfaces.* This reaction would be favored on the unpromoted Ag surface involved here, as verified by the low selectivity (12%) of an Ag/η-Al_2O_3 catalyst very similar to this one (*47*).

The presence of an adsorbed acetate species on Ag accounts for only one of the peaks in the carboxylate region. The assignment of a specific peak to the acyl carbon of the acetate group is supported by the CP/MAS spectrum for silver acetate powder shown in Fig. 5. In this spectrum, the chemical shift for the carboxyl carbon is 178 ppm, which is near the value of 180 ± 1 ppm observed for the Ag/Al_2O_3 samples. This assignment is consistent with the behavior of the peak intensity upon heating. The peak grew slightly more intense upon heating to 523 K, but diminished considerably, though not completely, at 573 K, while the other carboxylate peaks vanished at this temperature (see Fig. 8). This indicates that the acetate is the most stable of the carboxylate species observed consistent with results of Barteau *et al.* (*35*). Elevated temperatures appear to enhance formation of carboxyl-containing species, including an adsorbed acetate species via the reaction of ethylene and adsorbed oxygen; however, the carboxylates begin to decompose at temperatures above 523 K, and presumably their formation is no longer possible due to the absence of C_2H_4. This evidence for carboxylate formation at elevated temperature is consistent with the result reported by Anderson *et al.* (*40*) that the heat of adsorption of C_2H_4 on oxygen-covered Ag increased from 5.2 kcal/mol at 300 K to 64 kcal/mol at 443 K, because the latter value implies a strong interaction with the surface, i.e., the formation of a partially oxidized intermediate. Any CO_2 or atomic carbon residue formed above 523 K may not be detected by cross polarization if the carbon residue is too distant from protons or if CO_2 is in the gas phase. Their formation would explain the overall loss in signal detection in Fig. 8d. Such a carbon residue is anticipated not only because insufficient oxygen is present for complete oxidation to CO_2 and H_2O, but also because acid sites on the alumina can catalyze polymerization of ethylene.

The temperature required for the onset of acetate decomposition is consistent with the work of Madix and co-workers because their results suggest that decomposition is enhanced by the presence of adsorbed oxygen. Barteau *et al.* found that acetate species decomposed at 640 K on a Ag(110) surface covered by 0.1 monolayer of oxygen (*35*), but Sault and Madix reported that the decomposition temperature was lowered to 580 K on a Ag(110) surface with 0.5 monolayer of preadsorbed oxygen and, in the presence of 0.7 Torr of gas-phase oxygen, the acetate decomposed at temperatures as low as 400 K (*48*). The latter result was attributed to the reaction of this acetate complex with adsorbed oxygen atoms to form an adsorbed formate species, which decomposed at 410 K. In the presence of excess C_2H_4, i.e., higher C_{AD}/O_{AD} ratios, we do not observe formation of formate or carbonate species on the Ag surface (Fig. 8); however, at lower C_{AD}/O_{AD} ratios these two species are also present on the Ag surface (Fig. 4). Thus C–C bond rupture is favored at low coverages of strongly bound C_2H_4 on O-covered Ag.

A formate group adsorbed on Ag is a strong candidate to account for one of the resonances in the carboxylate region. In the liquid phase, the acyl carbon resonance in

formic acid, HCOOH (δ = 166.5 ppm), is shifted upfield with respect to that in acetic acid, CH_3COOH (δ = 175.7 ppm). This is consistent with the position of the peaks at 164 ppm (Fig. 4) with respect to the acetate resonance (δ = 180 ppm) and with the isotropic chemical shift of 164 ppm reported for solid ammonium formate (*25*). Thus our results support the proposal of Madix and co-workers that a formate species is present during acetate decomposition (*35, 48, 49*). However, the results of the interrupted decoupling experiments clearly show that no resonances originating from immobilized, protonated carbons were observed. Since the carboxy carbon in formate bears a proton, the proposed formate species would have to possess molecular motion or mobility on the surface to validate this result. Formate species adsorbed on Ag decompose near 410 K (*48, 49*), which eliminates the peak at 161 ppm as a candidate since its intensity does not change after heating at 523 K and supports its assignment to an oxalate species. Since reversibly adsorbed C_2H_4 was absent in the 6.7% Ag/Al_2O_3(O-E) sample, the ratio of surface sites coordinated with adsorbed oxygen to C atoms in $(C_2H_4)_{AD}$ was greater than 2. The greater amount of oxygen allowed the formation of formate species via partial oxidation of adsorbed acetate, possibly by the mechanism proposed by Sault and Madix (*48*). The presence of an oxalate species, as indicated by the peak at 160 $\pm$ 1 ppm, supports the IR assignment made by Force and Bell (*7*) and, as they proposed, it is expected to be an intermediate associated with complete combustion to CO_2 and H_2O. Finally, the assignment of the peak at 170 ppm to a surface carbonate species is consistent with the IR spectra reported by Force and Bell as they observed peaks for both monodentate and bidentate carbonate species (*7*). Again, this carbonate group is associated with complete combustion. Of these various groups associated with complete combustion, the results in Fig. 8 indicate that acetate and oxalate species are preeminent.

The Al_2O_3 could also provide adsorption sites for carboxyl-containing species. The carboxylate resonances are absent in the CP/MAS spectrum of pure Al_2O_3(R), as indicated in Fig. 7a, which is consistent with the proposal that carboxylate formation occurs via a Ag-catalyzed oxidation reaction. However, for Ag/Al_2O_3, the possibility exists that acetate and formate species can migrate from the Ag to the Al_2O_3 surface and adsorb on Brønsted-acid sites (*31*). Several workers have used NMR to study the adsorption of compounds containing carbonyl groups on oxide materials (*50–52*). The acyl carbon in acetone has been shown to interact strongly with hydroxyl groups on SiO_2 yielding downfield shifts up to 10 ppm for the carbonyl resonance relative to the liquid state (*50, 51*). However, in these three studies, adsorption was weak and the species were mobile since the resonances could be observed in the presence of the gas phase without magic-angle spinning. In contrast, the carboxylate resonances in our study were observed only under MAS conditions and were not removed by evacuation at 298 K for 24 h; moreover, the carboxylate species were stable upon heating to 523 K. The evidence presented here indicates that adsorption on Al_2O_3 is weak compared to that on Ag and that the carboxylate resonances originate from species bound strongly to the Ag surface; however, the possibility of adsorption on the Al_2O_3 cannot be completely discounted, especially if acetaldehyde is formed, and one or two of the bands between 160 and 180 ppm could possibly represent such species.

Distinct peaks at 28 and 13 ppm and a weak band near 61 ppm appear in the spectrum for pure Al_2O_3 (see Fig. 7). The chemical shifts suggest the presence of alkoxy species on the Al_2O_3 surface, such as $Al–O–CH_2–CH_3$ and $Al–O–CH_2–(CH_2)_2–CH_3$, which are most likely associated with adsorption on Brønsted-acid sites (*31*). These species are consistent with the known chemical shifts of model liquid-phase compounds (*27*). Using proton NMR of deuter-

ated pyridine adsorbed on Al_2O_3, Pearson measured weak Brønsted acid sites whose concentration increased as evacuation temperatures increased up to 973 K (*53*). Moreover, species analogous to the alkoxy species above have been reported to be formed from the adsorption of acetylene on γ-Al_2O_3 at 300 K (*54*) and on an HZSM-5 zeolite at elevated temperatures (*55*). In both cases Al–O–CH=CH_2 was formed.

The appearance of peaks at 35 and 8 ppm after heating (see Fig. 8) suggests that ethylene oligomerization may occur at elevated temperatures, along with the possible formation of ethane since the chemical shift of ethane is 6.5 ppm (*27*). Van den Berg *et al.* have associated a ^{13}C peak near 35 ppm with aliphatic C atoms formed during ethylene oligomerization at 300–337 K on Brønsted–acid sites of an HZSM-5 zeolite (*56, 57*). Their mechanism for ethylene oligomerization involved alkoxy species, and a similar mechanism has also been proposed for propylene oligomerization on HZSM-5 (*58*).

SUMMARY

NMR can provide valuable information about the surface species formed after adsorption of C_2H_4 on supported Ag crystallites. On oxygen-covered Ag, a more strongly bound state of C_2H_4 exists as well as a weakly bound (reversibly adsorbed) state, while on reduced Ag all the C_2H_4 is weakly adsorbed. The NMR resonance of irreversibly adsorbed C_2H_4 on O-covered Ag exhibits the greatest upfield shift relative to gas phase C_2H_4 (-20 ppm). A smaller upfield shift and narrower linewidth for reversibly adsorbed C_2H_4 is consistent with a weaker interaction with the Ag surface. Both adsorbed states of C_2H_4 exhibit surface mobility, and both the surface mobility and the chemical shift data suggest rapid exchange between the two adsorbed states.

On oxygen-covered Ag, C_2H_4 reacts with surface oxygen atoms to form stable carboxylate species. Acetate and oxalate species are observed in the presence of weakly adsorbed C_2H_4 after successively higher temperatures are attained. In the presence of only irreversibly adsorbed C_2H_4 on an O-covered surface, formate and carbonate species also appear to be formed; thus C–C bond breaking seems to be favored under these latter conditions. Formation of the carboxylate species is enhanced by heating to 523 K, but their disappearance occurs at 573 K after the adsorbed ethylene has reacted away. *Acetate and oxalate species on the Ag appear to be the principal intermediates associated with the complete combustion of ethylene.* A small amount of C_2H_4 also adsorbs on Al_2O_3 and exhibits a chemical shift near that of gas-phase C_2H_4. Chemical shifts of other resonances indicate the formation of alkoxy species on Brønsted acid sites on the Al_2O_3 surface, and at elevated temperatures some C_2H_4 oligomerization may also occur on these sites.

ACKNOWLEDGMENTS

The initial part of this study was begun under NSF Grant CBT-840665. The final part was sponsored by a Texaco Foundation Fellowship.

REFERENCES

1. van Santen, R. A., and Kuipers, H. P. C. E., *in* "Advances in Catalysis" (D. D. Eley, H. Pines, and P. B. Weisz, Eds.), Vol. 35, p. 265. Academic Press, New York, 1987.
2. Berty, J. M., *in* "Applied Industrial Catalysis" (B. E. Leach, Ed.), Vol. 1, p. 207. Academic Press, New York, 1983–1984.
3. Sachtler, W. M. H., Backx, C., and van Santen, R. A., *Catal. Rev.-Sci. Eng.* **23,** 127 (1981).
4. Verykios, X. E., Stein, F. P., and Coughlin, R. W., *Catal. Rev.-Sci. Eng.* **22,** 197 (1980).
5. Kilty, P. A., and Sachtler, W. M. H., *Catal. Rev.-Sci. Eng.* **10,** 1 (1974).
6. Sachtler, W. M. H., *Catal. Rev.-Sci. Eng.* **4,** 27 (1970).
7. Force, E. L., and Bell, A. T., *J. Catal.* **38,** 440 (1975).
8. Force, E. L., and Bell, A. T., *J. Catal.* **40,** 356 (1975).
9. Mehring, M., *Z. Phys. Chem.* **151,** 1 (1987).
10. Mostikhin, V. M., and Zamaraev, K. I., *Z. Phys. Chem.* **152,** 58 (1987).
11. Wang, P-K., Ansermet, J-P., Rudaz, S. L., Wang, Z., Shore, S., Slichter, C. P., and Sinfelt, J. H., *Science* **234,** 35 (1986).
12. Nagy, J. B., Engelhardt, G., and Michel, D., *Adv. Colloid Interface Sci.* **23,** 67 (1985).

13. Maciel, G. E., *in* "Heterogeneous Catalysis" (B. L. Shapiro, Ed.), p. 349. Proc. 2nd Symp. IUCCP, Dept. Chem., Texas A&M Univ., 1984.
14. Duncan, T. M., and Dybowski, C., *Surf. Sci. Rep.* **1,** 157 (1981).
15. Pfeiffer, H., *Phys. Rep.* **26,** 293 (1976).
16. Derouane, E. G., Fraissard, J., Fripiat, J. J., and Stone, W. E. E., *Catal. Rev.* **7,** 121 (1972).
17. Pruski, M., Kelzenberg, J. C., Gerstein, B. C., and King, T. S., *J. Am. Chem. Soc.* **112,** 4232 (1990).
18. Gay, I. D., *J. Catal.* **108,** 15 (1987).
19. Plischke, J. K., and Vannice, M. A., *Appl. Catal.* **42,** 255 (1988).
20. Seyedmonir, S. R., Strohmayer, D. E., Geoffroy, G. L., and Vannice, M. A., *Adsorpt. Sci. Technol.* **1,** 253 (1984).
21. Chen, A., Kaminsky, M., Geoffroy, G. L., and Vannice, M. A., *J. Phys. Chem.* **90,** 4810 (1986).
22. Plischke, J. K., Ph.D. thesis, The Pennsylvania State University, 1990.
23. Scholten, J. J. F., Konvalinka, J. A., and Beekman, F. W., *J. Catal.* **28,** 209 (1973).
24. Czanderna, A. W., *J. Phys. Chem.* **68,** 2765 (1964).
25. Duncan, T. M., "A Compilation of Chemical Shift Anisotropies." Farragut Press, Chicago, 1990.
26. Chin, Y-H., and Ellis, P. D., *J. Am. Chem. Soc.*, in press.
27. Breitmaier, E. and Voelter, W., *in* "Carbon-13 NMR Spectroscopy. High Resolution Methods and Applications in Organic Chemistry and Biochemistry," 3rd ed., p. 192. VCH, Weinheim, Germany, 1987.
28. Denney, D., Mastikhin, V. M., Namba, S., and Turkevich, J., *J. Phys. Chem.* **82,** 1752 (1978).
29. Mudrakovskii, I. L., Mastikhin, V. M., Bogdanchikova, N. E., and Khasin, A. V., *React. Kinet. Catal. Lett.* **34,** 185 (1987).
30. Opella, S. J., and Frey, M. H., *J. Am. Chem. Soc.* **101,** 5854 (1979).
31. Anderson, J. R., *in* "Structure of Metallic Catalysts," p. 46. Academic Press, London, 1975.
32. Gerei, S. V., Kholyavenko, K. M., and Rubanik, M. Y., *Ukrain. Khim. Zh.* **31,** 449 (1975).
33. Kilty, P. A., Rol, N. C., and Sachtler, W. M. H., *in* "Proceedings 5th International Congress on Catalysis, Palm Beach, 1972" (J. W. Hightower, Ed.), Paper 64, p. 929. North-Holland, Amsterdam, 1973.
34. Kanno, T., and Kobayashi, M., *in* "Proceedings, 8th International Congress on Catalysis, Berlin, 1984," Vol. III, p. 277. Dechema, Frankfurt am Main, 1984.
35. Barteau, M. A., Bowker, M., and Madix, R. J., *J. Catal.* **67,** 118 (1981).
36. Meiler, W., Weller, Th., Lochmann, R., and Michel, D., *Chem. Phys.* **82,** 379 (1983).
37. Michel, D., Meiler, W., and Pfeifer, H., *J. Mol. Catal.* **1,** 85 (1975/1976).
38. Michel, D., Meiler, W., and Hoppach, D., *Z. Phys. Chem. (Leipzig)* **255,** 509 (1974).
39. Takasugi, M., Watanabe, N., and Ujihira, Y., *Fresenius' Z. Anal. Chem.* **315,** 502 (1983).
40. Anderson, K. L., Plischke, J. K., and Vannice, M. A., *J. Catal.* **128,** 148 (1991).
41. Campbell, C. T., and Paffett, M. T., Appl. Surf. Sci. *19,* 28 (1984).
42. Jelinski, L. W., and Melchior, M. T., *in* "Practical Spectroscopy. NMR Spectroscopy Techniques" (C. Dybowski and R. L. Lichter, Eds.), Vol. 5, Chap. 6, p. 253. Dekker, New York, 1987.
43. Twigg, G. H., *Trans. Faraday Soc.* **42,** 284 (1946).
44. Ide, Y., Takagi, T., and Keii, T., *Nippon Kagaku Kasshi* **86,** 1249 (1965).
45. Kenson, R. E., and Lapkin, M., *J. Phys. Chem.* **74,** 1493 (1970).
46. Grant, R. B., and Lambert, R. M., *J. Catal.* **93,** 92 (1985).
47. Seyedmonir, S. R., Plischke, J. K., Vannice, M. A., and Young, H. W., *J. Catal.* **123,** 534 (1990).
48. Sault, A. G., and Madix, R. J., *J. Phys. Chem.* **90,** 4723 (1986).
49. Barteau, M. A., Bowker, M., and Madix, R. J., *Surf. Sci.* **94,** 303 (1980).
50. Gay, I. D., *J. Phys. Chem.* **78,** 38 (1974).
51. Bernstein, T., Michel, D., Pfeifer, H., and Fink, P., *J. Colloid Interface Sci.* **84,** 310 (1981).
52. Enriquez, M. A., and Fraissard, J. P., *J. Catal.* **74,** 89 (1982).
53. Pearson, R. M., *J. Catal.* **46,** 279 (1977).
54. Chin, Y-H., and Ellis, P. D., *J. Am. Chem. Soc.* **111,** 7653 (1989).
55. Lazo, N. D., White, J. L., Munson, E. J., Lambregts, M., and Haw, J. F., submitted for publication.
56. van den Berg, J. P., Wolthuizen, J. P., Clague, A. D. H., Hays, G. R., Huis, R., and van Hooff, J. H. C., *J. Catal.* **80,** 130 (1983).
57. van den Berg, J. P., Wolthuizen, J. P., and van Hooff, J. H. C., *J. Catal.* **80,** 139 (1983).
58. Haw, J. F., Richardson, B. R., Oshiro, I. S., Lazo, N. D., and Speed, J. A., *J. Am. Chem. Soc.* **111,** 2052 (1989).